FIBRE LASER WELDING OF DUAL PHASE STEELS

Pavol Švec[1)*], Alexander Schrek[1)], Viliam Hrnčiar[1)], Tomáš Csicsó[1)]
[1)] Institute of Technologies and Materials, Faculty of Mechanical Engineering, Slovak University of Technology in Bratislava, Bratislava, Slovakia

[*] Corresponding author: *e-mail: pavol.svec@stuba.sk, Tel.: +421 905211336, Institute of Technologies and Materials, Faculty of Mechanical Engineering, Slovak University of Technology in Bratislava, Pionierska 15, 831 02 Bratislava*

Abstract

The fibre laser welding of two different dual phase steels HCT980X and HCT600X was evaluated. The sheets with thickness of 1.2 mm were welded using the solid-state fibre laser IPG type YLR 4500 with maximum output 4.5 kW and wave length 1060 nm at graduated beam powers and welding speeds. The microstructure of welded samples was analysed, microhardness and tensile strength were measured. The heat input influenced the microstructure of the fusion zone and heat affected zone. The microhardness increased in the fusion zone and even more in the heat affected zone of HCT980X steel, which was the consequence of martensite and bainite formation in these areas. The tensile strength of joints achieved the strength of the HCT600X steel and all joints fractured in the HCT600X base metal.

Keywords: dual phase steels, fibre laser welding, microstructure, microhardness, tensile strength

1 Introduction

Dual phase (DP) steels, which are the important part of advanced high strength steels, have been used in manufacture of lightweight automobiles to reduce fuel consumption without compromising other attributes such as safety, performance, recyclability and cost. Some of the major advantages of the dual phase steels include their superior mechanical properties in comparison with standard steels, moderate price thanks to small amount of alloying additions, as well as excellent technological properties, together with good weldability and machinability [1-4]. The excellent mechanical properties are the consequence of their multiphase structure. Microstructure of DP steel consists of 30-70 % martensite in the fine-grained, spherical ferrite matrix and 1-10 % of metastable retained austenite. As a result, the steel is characterised by high tensile strength up to 1180 MPa with unit elongation up to 27 %. Most often the microstructure of DP steel is developed as a result of accelerated cooling of thin sheets after cold rolling in the range between A_{c1} and A_{c3} and controlled air-water mist cooling to ambient temperature. The process is flexible one and allows for different combinations of relative volume ratio of ferrite and martensite. The dual phase steels are used in automotive industry for frames and crossbeams, vertical beams, side impact beams, and safety elements [4-6].

Dual phase steels have been used for producing of tailor welded blanks. Tailor welded blanks are semi-finished parts that consist of at least two single sheets that are welded together prior the forming process. The sheets can exhibit different mechanical properties, thickness or coatings.

In series production the joining of the blanks is usually done by laser welding though other weld techniques are also possible [7-10]. Using tailor welded blanks enable an adaptation to locally different loading conditions or other requirements in the part. Other advantage of joining prior to the forming is the reduction of the number of the required forming tools, the higher accuracy in the forming process and the enhanced use of material which leads to less production costs. The most important advantage of part made from tailor welded blanks is the weight reduction compared to conventional products. A car body manufactured using tailor welded blanks and high strength steels can achieve a 25 % weight reduction [10-12].

Laser welding process has been widely used for creating of tailor welded blanks due to the small heat-affected zone (HAZ) and fusion zone (FZ), the lover cost and greater flexibility compared to other welding methods. Although the laser welding process produces less impact on the material properties than others, the tailor-welded blanks formability is worsened by material properties resulting from microstructure changes accompanying the laser welding. The microstructure is affected mainly by chemical composition of base materials, sheets thickness and welding parameters such as power input, welding speed and others. The final microstructure in FZ and HAZ weld is consequence of rapid heating and cooling cycles with melting and solidification happening in a significantly short time. FZ and HAZ are characterised by increased hardness and decreased plastic properties. The welding parameters influence also the weld imperfections, which are related to the weld geometry such as concavity, impurities or gaseous elements, porosity, pinholes or craters. Optimization of welding parameters is useful to accomplish the required microstructure of welds in tailor welded blanks [13-16].

2   Experimental procedures

Two different dual-phase steel sheets HCT980X Z100MBO and HCT600X Z100MBO with thickness of 1.2 mm and zinc coating of 100 g.m^{-2} were used for laser welding. The chemical composition of the experimental steels is given in **Tab. 1** and their mechanical properties are given in **Tab. 2**. Used dual phase steels differ in contents of carbon and manganese, maximal allowed concentration of others elements is the same (**Tab. 1**).The HCT980X grade dual phase steel has higher amount of these elements which is the consequence of higher strength and lower plasticity in comparison with HCT600X grade dual phase steel (**Tab. 2**). The maximal concentration of Al (2.0 %) given in standards for both steels is quite high, but the typical concentration is0.04 % Al.

Table 1 Maximal concentration of alloying elements in dual phases steels [wt. %]

Steel	C	Mn	Si	Al	P	S	V	B	Cr + Mo	Nb + Ti
HCT600X	0.17	2.2	0.8	2.0	0.08	0.015	0.2	0.05	1	0.15
HCT980X	0.23	2.5	0.8	2.0	0.08	0.015	0.2	0.05	1	0.15

Table 2 Mechanical properties of dual phase steels

Steel	Tensile strength R_m [MPa]	Proof strength $R_{p0.2}$ [MPa]	Elongation A_{80} [%]
HCT600X	600	340 - 420	min. 20
HCT980X	980	600 -750	min. 10

The welding experiments were done on the solid-state fibre laser IPG type YLR 4500 with maximum output 4.5 kW, wave length 1060 nm and fibre diameter 100 µm. Welding

experiments were conducted on sheets with length of 200 mm and width of 100 mm along the longitudinal edge. Prior to welding abutting surfaces were cleaned with steel wire brush followed by acetone swabbing. The butt joints were prepared at six different beam power (P), welding speeds (v) and calculated heat input values (P/v). The distance of welding head was 250 mm, and focal position was 10 mm at all samples and samples were prepared without filler metal and without shield atmosphere. The variable welding parameters are summarized in **Tab. 3**.

Table 3 Parameters of fibre laser welding

Weld No	Beam power [W]	Welding speed [mm.s^{-1}]	Heat input [J.mm^{-1}]
1	550	5	110
2	900	10	90
3	1500	30	50
4	2200	50	44
5	2760	70	39,4
6	4300	100	43

The macrostructures of the laser weld surfaces prepared with different welding parameters were observed on the stereomicroscope Zeiss. The microstructure was studied on samples cut off the welding joints and prepared using standard metallographic techniques. The microstructures were observed using Axiovert 40MAT light microscope and JEOL 6010 scanning electron microscope. Microhardness surveys were performed on transverse sections of weld bead centres parallel to the surfaces of sheets using Vickers indent or according to the EN ISO 6507-1 standard. The samples for tensile tests were prepared from welded joints and tests were carried out using universal testing machine Instron 195 at room temperature according to the EN ISO 6892-1 standard.

3   Results

Tab. 4 shows the macrostructures of the laser weld surfaces prepared with different welding parameters. The different bead pool widths can be seen in these welds. Increased welding speed and beam power were the consequence of smaller amount of the heat input and were accompanied with decreasing of the weld width, but more intensive splash and creating of small pinholes on the root side of the weld. The bead pool prepared at the maximal speed of 100 mm.s^{-1} was the thinnest one and also smoothest one in comparison to the joints welded at the lower speeds.

Fig. 1, 2 and **3** show laser weld cross sections of the joints prepared at welding speeds of 5, 30 and 100 mm.s^{-1}, respectively. Sections of fusion zones (FZ) and heat affected zones (HAZ) can be distinguished. As can be seen the welds are well formed and free of porosity or cracks in the FZ. The joints are characterised with the concavity of the face and root sagging. The width of both FZ and HAZ decrease with increasing of the welding speed and the highest difference can be seen when comparing joints welded at speeds of 5 and 100 mm.s^{-1}.

Table 4 Macrostructure of the bead pool of laser joints welded at different parameters

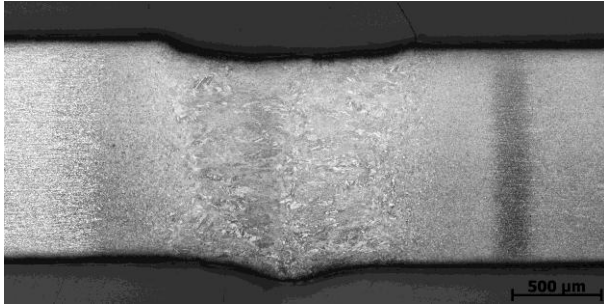| No	Face of the weld	Root of the weld
1		
2		
3		
4		
5		
6		5 mm
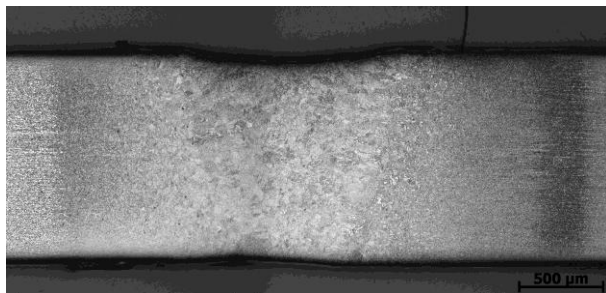
Fig. 1 Cross section of the but joint prepared at welding speed of 5 mm.s⁻¹

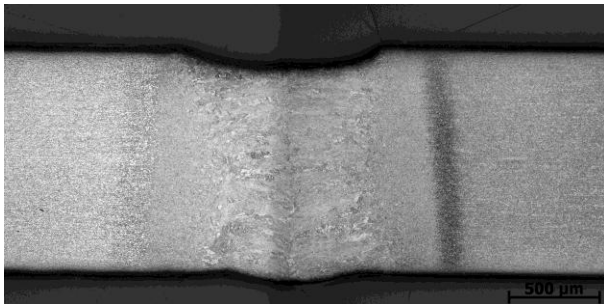**Fig. 2** Cross section of the but joints prepared at welding speed of 30 mm.s^{-1}

Fig. 3 Cross section of the but joint prepared at welding speed of 100 mm.s^{-1}

The microstructures of dual phase steels are shown in **Fig. 4** and **5**. The microstructures of both steels consist of the same phases, martensitic island in ferrite matrix, but with different relative volume of martensite and ferrite and average grain size. According to the work [17] the HCT600X DP steel consists of 75 % of martensite, 24 % of ferrite and 1 % of retained austenite, and HCT980X DP steels consist of 50 % of martensite, 49 % of ferrite and 1 % of retained austenite. The average grain size was measured by the image analysis and is from 7 to 13 µm for HCT600X steel and from 500 nm to 1 µm for HCT980X DP steel.
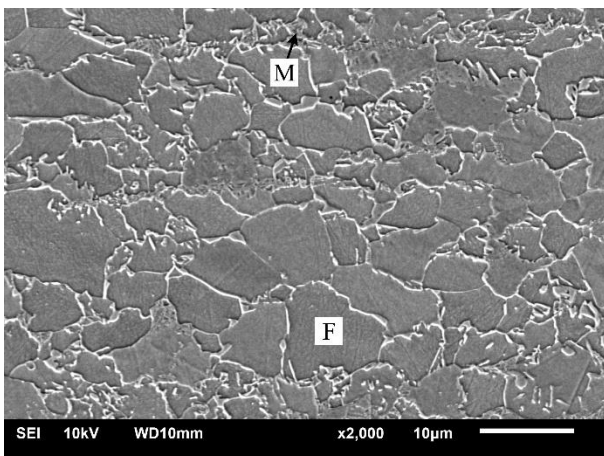
Fig. 4 Microstructure of the dual phase steel HCT600X (M – martensite, F – ferrite)
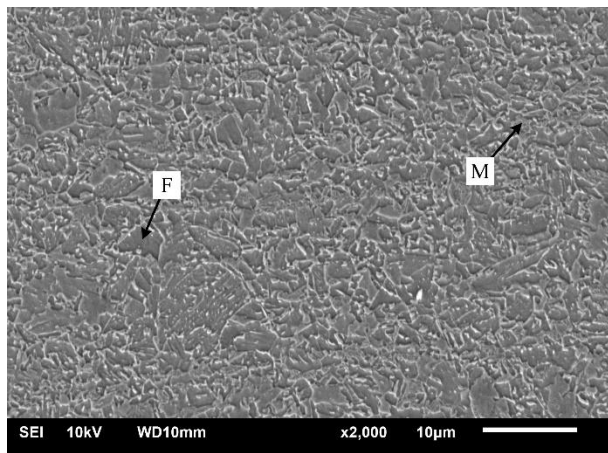
Fig. 5 Microstructure of the dual phase steel HCT980X (M – martensite, F – ferrite)

Fig. 6 and **7** show the microstructures of FZ of laser weld of dual phase steels. The microstructures in FZ are the results of solidification behaviour and subsequent solid phase transformation, which are controlled by composition and heat input. The laser weld zone includes various microstructural constituents and larger number of lath shaped and acicular structures. Large areas of the coarse ferrite and acicular ferrite were found in the FZ of the weld joints, as it is shown in **Fig. 6**. The smaller areas, shown in **Fig. 7**, were created by the lath microconstituents. Laths of martensite or bainite were built in packets and were the consequence of rapid cooling.
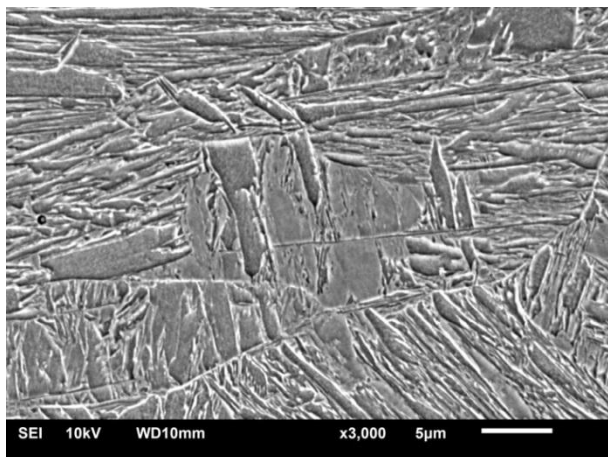

Fig. 6 Ferrite and acicular ferrite in FZ of weld

The microstructures of HAZ in **Fig. 8** and **9** were created under the effect of thermal weld cycle. As the chemical compositions of both DP steels are similar and they differ only slightly in the content of carbon and manganese, the microstructure of both HAZ is similar. The microstructures are composed of a mixture of ferrite, bainite and martensite, which are built in packets. The microstructures of HAZ near both base metals HCT980X and HCT600X were finer than the microstructures of HAZ near the FZ, which were coarser.
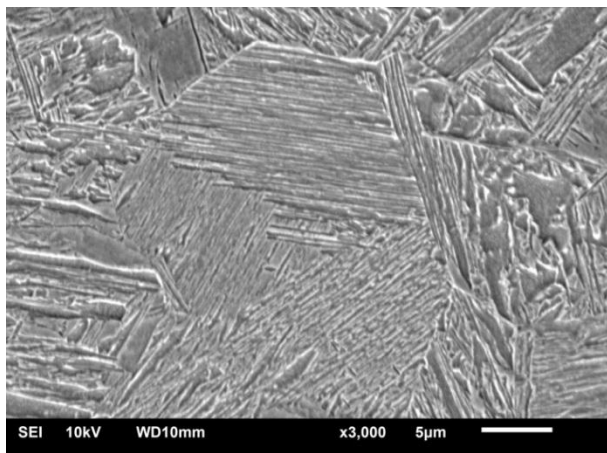
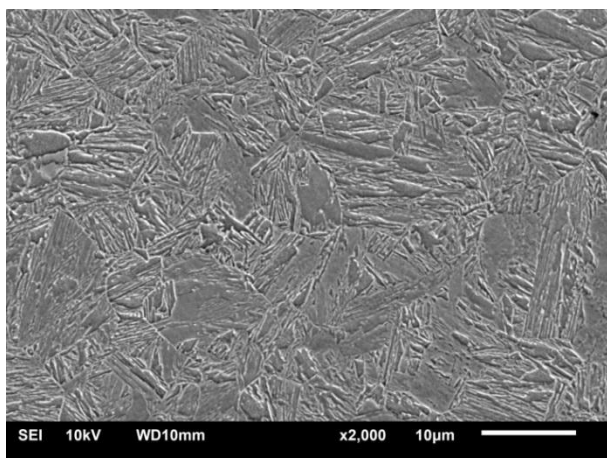**Fig. 7** Lath microconstituents in FZ of weld

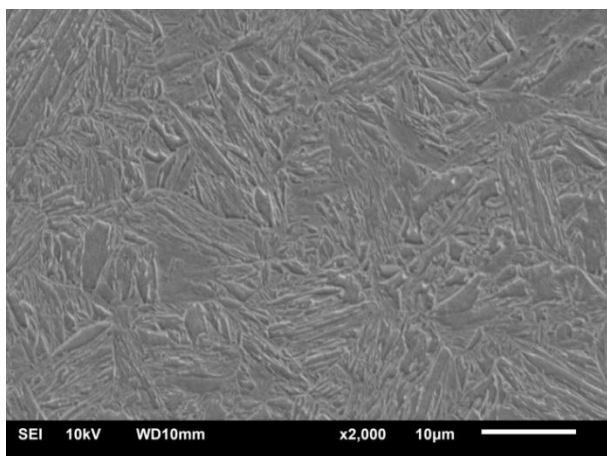**Fig. 8** The microstructures of HAZ near the HCT600X steel

Fig. 9 The microstructures of HAZ near the HCT980X steel

The quantitative chemical compositions of BM and FZ were measured by energy dispersive spectroscopy and confirmed the higher concentration of alloying element in HCT980X steel (2.4 % Mn) in comparison to HCT600X steel (1.9 % Mn). Measured values were in good agreement with the values in the **Tab. 1**. The concentration of manganese in the FZ (2.2 % Mn) of these dual phase steels was in the interval of these two base metals. The concentration of others measured alloying elements was the same in both base metals and also in the FZ (0.5 % Cr, 0.2 % Si).
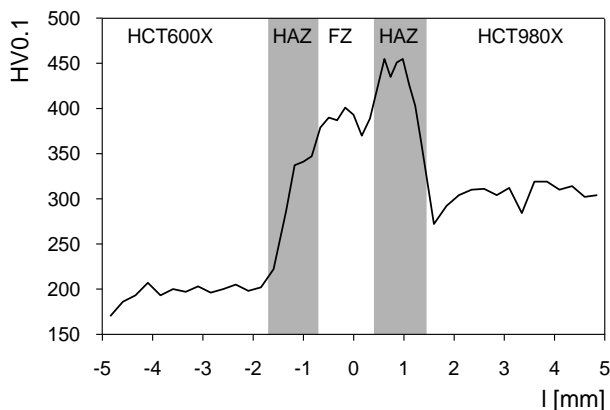

Fig. 10 Microhardness across the joint prepared at welding speed of 5 mm.s^{-1}

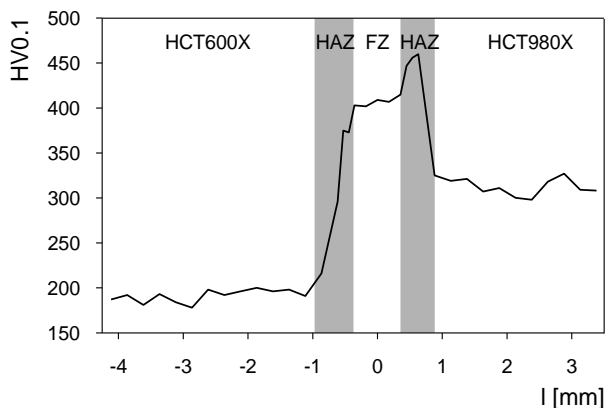**Fig. 11** Microhardness across the joint prepared at welding speed of 100 mm.s^{-1}

Different values of microhardness across the joints were measured (**Fig. 10** and **11**), although different welding parameters had the small effect on the maximal measured hardness values in the different areas (BM, FZ and HAZ). Only slightly higher values in these areas were measured in the weld prepared at the largest speed of 100 mm.s^{-1}(**Fig. 11**) in comparison to the sample with the welding speed of 5 mm.s^{-1}(**Fig. 10**). The width of FZ and both HAZ was larger at the minimal welding speed (the largest heat input) and thinner at the maximal welding speed (the smallest heat input). The hardness in the HCT600X steels was about 220HV0.1 and 330HV0.1 in the HCT980X steel for all joints. The maximal microhardness in HAZ of HCT600X was 380 HV0.1 and in HAZ of HCT980X was 460 HV0.1, which was the highest measured

microhardness. The hardness in the FZ of all samples was in the interval of $370 \div 420$ HV0.1. The maximal hardness of 420 HV0.1 was achieved at highest welding speed of 100 mm.s^{-1}(**Fig. 11**) and consequently the lowest heat input and largest cooling speed. The measured values are in good agreement with work of [17]. In this work average microhardness of ferrite was 220HV0.1 and of martensite 384HV0.1 for HCT600X DP steel. Microhardness of ferrite was 225HV0.1 and of martensite 415HV0.1 for HCT980X DP steel. These values confirm the identification of microstructural constituents.

The tensile test showed that the weld metal strength was much higher than the tensile strength of weaker steel HCT600X and it was in line with the microhardness results. The Sample before the tensile test and typical fracture of sample after the tensile test are presented in **Fig. 12**. It can be seen that the fractures occurred away from the FZ and HAZ. The average strength of tensile samples was at the same level as that of the base metal, and equalled 670 MPa.
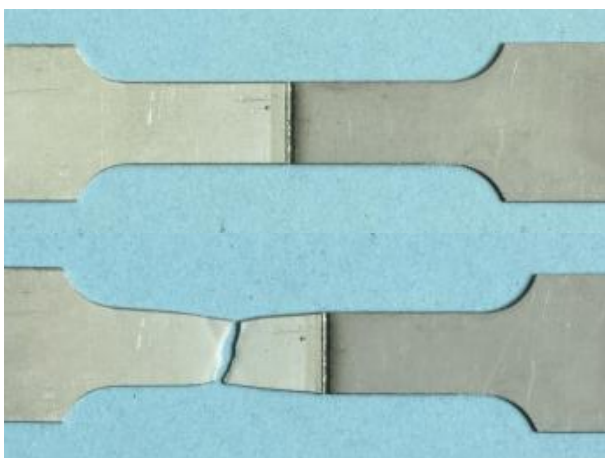

Fig. 12   The tensile samples before and after the tensile test

Conclusions

The fibre laser welding of two different dual phase steels HCT980X and HCT600X was studied. The effects of beam power and welding speed on microstructure, microhardness and tensile strength of laser welds was evaluated. The structural examination of the weld cross section revealed that the welds were free of porosity or cracks and their geometry was characterised with slight concavity of the face and root sagging. These imperfections didn't have the negative effect on the tensile strength of the joints. Large areas of the coarse ferrite and acicular ferrite were found in the FZ of the weld joints. The smaller areas were created by the lath microconstituents. Laths of martensite or bainite were built in packets and were the consequence of rapid cooling. The microstructure in the FZ included a larger number of lath-shaped and acicular structures and was coarser than the one in heat affected zone. The microstructures of both HAZ consisted of ferrite, martensite and bainite. The different values of hardness across BM, FZ and HAZ were observed and were caused by rapid solidification and cooling of these zones. The weld metal strength was higher than the BM strength and all joints fractured in the BM. Results of fibre laser welding confirm proper quality of joints prepared at tested parameters.

References

[1] M. Merklein, M. Johannes, M. Lechner, A. Kuppert: Journal of Materials Processing Technology, Vol. 214, 2014, No. 2, p. 151-164, DOI:10.1016/j.jmatprotec.2013.08.015

[2] D. Dong, Y. Liu, Y. Yang, J. Li, M. Ma, T. Jing: Materials Science & Engineering A, Vol. 594, 2014, No. 1, p. 17-25, DOI:10.1016/j.msea.2013.11.047

[3] K. Kocúrová, M. Dománková, M. Hazlinger: Metalurgija, Vol. 52, 2013, No. 1, p. 19-22

[4] D. Yan, C.C. Tasan, D. Raabe: Acta Materialia, Vol. 96, 2015, p. 399-409, DOI:10.1016/j.actamat.2015.05.038

[5] M. Rossini, P. Russo Spena, L. Cortese, P. Matteis, D. Firrao: Materials Science & Engineering A, Vol. 628, 2015, p. 288-296, DOI:10.1016/j.msea.2015.01.037

[6] L. Schemmann, S. Zaefferer, D. Raabe, F. Friedel, D. Mattissen: Acta Materialia, Vol. 95, 2015, p. 386-398, DOI: 10.1016/j.actamat.2015.05.005

[7] Q. Wu, J. Gong, G. Chen, L. Xu: Optics Laser Technology, Vol. 40, 2008, No. 2, p.420-426, DOI:10.1016/j.optlastec.2007.06.004

[8] A.K. Sinha, D.Y. Kim, D. Ceglarek: Optics and Laser in Engineering, Vol. 51, 2013, No. 10, p. 1143-1152, DOI:10.1016/j.optlaseng.2013.04.012

[9] L. Mei, G. Chen, X. Jin, Y. Zhang, Q. Wu: Optics Laser Technology, Vol. 47, 2009, No. 11, p. 1117-1124, DOI:10.1016/j.optlaseng.2009.06.016

[10] X. Fengxiang, S. Guangyong, L. Guangyao, L. Qing: Journal of Materials Processing Technology, Vol. 214, 2014, p. 925-935, DOI:10.1016/j.jmatprotec.2013.11.018

[11] J. Viňáš, Ľ. Kaščák, D. Draganovská: Acta Metallurgica Slovaca,Vol. 18, 2012, No. 4, p. 162-171

[12] M. Sokolov, A. Salminen, M. Kuznetsov, I. Tsibulskiy: Materials and Design, Vol. 32, 201, No. 10, p. 5127-5133, DOI:10.1016/j.matdes.2011.05.053

[13] J. Meško, A. Zrak, K. Mulczyk, S. Tofil: Manufacturing Technology, Vol. 14, 2014, No. 3 p. 355-359.

[14] D.C. Saha, D. Westerbaan, S.S. Nayak, E. Biro, A.P. Gerlich, Y. Zhou: Materials Science & Engineering A, Vol. 607, 2014, p. 445-453, DOI:10.1016/j.msea.2014.14.034

[15] M. Marônek, J. Bárta, K. Bártová: Journal of ASTM International, Vol. 9, 2012, No. 2, p. 197-208, DOI: 10.1520/JAI103375

[16] Y. Mazaheri, A. Kermanpur, A. Najafizadeh: Materials Science & Engineering A, Vol. 639, 2015, p. 8-14, DOI:10.1016/j.msea.2015.04.098

[17] S. Krajewski, J. Nowacki: Archives of Civil and Mechanical Engineering, Vol. 14, 2014, No. 2, p. 278-286, DOI:10.1016/j.acme.2013.10.002

Acknowledgements